JOURNAL OF SOLID STATE CHEMISTRY 38, 121–127 (1981)

Crystal Structure and Fast Ionic Conduction of $TlZrF_5$

D. AVIGNANT, I. MANSOURI, R. CHEVALIER, AND J. C. COUSSEINS*

Groupe de Cristallographie et de Chimie des Solides, ERA n° 897, Université de Clermont-Ferrand II, B.P. 45, 63170 Aubiere, France

Received October 31, 1980

$TlZrF_5$ crystallizes in the monoclinic system with unit cell dimensions $a = 8.112(1)$ Å, $b = 7.927(3)$ Å, $c = 7.929(1)$ Å, $\beta = 123.99(1)°$ and space group $P2_1/c$ (n° 14); $Z = 4$. The structure was solved by conventional Patterson and Fourier methods and refined by full-matrix least-squares techniques to a conventional R of 0.057 ($R_w = 0.063$). The structure consists of sheets of $(ZrF_5)^-$ that may be described as edge-shared and corner-shared bicapped trigonal prisms (ZrF_8). The sheets run parallel to the $y0z$ plane and are bonded together by the Tl ions which are surrounded by 12 F^- ions. The ionic conductivity of $TlZrF_5$ and $TlHfF_5$ has been investigated by complex impedance measurements and the relationships between structure and fast-ionic conduction are discussed.

Introduction

Recently some attention has been given to ionic conductivity in the fluorides with the fluorite-type structure, the tysonite-type structure, or both related structural types because of the high fluorine mobility in these materials (*1–12*).

These studies of the F^- ion conductivity in a large number of fluorides permit one to draw up some criteria responsible for high mobility of this anion (*13, 14*):

—low entropy of fusion,

—high cation polarizability,

—presence of cations having elevated coordination numbers.

Carrying out an exploratory program intended for the research of efficient materials we have extended these studies to new crystallographic phases which may be of interest in order to specify the role played by the structure, keeping in mind that by a suitable choice of cations (Tl for instance) it can easily meet the above criteria. We have attempted to augment the current experimental understanding of these compounds by conducting a systematic study of the transport properties due to the F^- ion in binary fluorides of monovalent thallium and tetravalent elements (M^{IV} = Th, U, Zr, Hf) and we report here the results of our investigations on $TlZrF_5$ and isostructural fluorides.

Experimental

Polycrystalline samples were prepared by reacting stoichiometric quantities of thallous fluoride and zirconium fluoride in platinum tubes sealed under dry argon gas. The samples were heated for 12 hr at 400°C and then cooled to room temperature slowly. The starting materials have been prepared in the laboratory. The thallous

* To whom all correspondence should be addressed.

0022-4596/81/070121-07$02.00/0

fluoride was obtained by incomplete neutralization of a 40% aqueous HF boiling solution by thallous carbonate and evaporated to dryness. The dry extract was ground and then heated for a few hours at 200°C under a dry nitrogen flow in order to remove the last traces of water and hydrofluoric acid. Both hafnium and zirconium tetrafluorides were prepared by direct fluorination of pure HfO_2 or ZrO_2 (Merck, selectipur) by heating in F_2 gas overnight at 500°C.

Crystals used in this study were grown from equimolar melts of TlF and ZrF_4 in sealed platinum tubes. The samples were heated for 4 or 5 hr at 480°C and cooled to room temperature at the rate of 4°C/hr. Clear colorless needlelike crystals were obtained, often twinned. They were identified as $TlZrF_5$ crystals by comparison between X-ray powder diffraction pattern of ground single crystals and that from a bulk preparation of $TlZrF_5$ reported previously (*15*).

Ionic conductivity measurements were made in the temperature range 50–260°C with an ac vector impedance meter (5 Hz to 500 kHz). Details of the conductivity equipment have been published elsewhere (*16*). The samples were pressed powder pellets sintered in sealed platinum tubes. The compactness of the sintered pellets was estimated from their weights and dimensions and found to be 0.84–0.86. The pellets were provided with sputtered gold or platinum paint electrodes (Leitplatin 308 A, Degussa) and spring loaded between platinum disks in a monel conducting cell. All experiments were carried out in a dry argon atmosphere.

Single-Crystal Diffraction Data

A small crystal was mounted along the *b* axis on a pyrex rod using Araldite. Preliminary Weissenberg and precession photographs showed the symmetry to be monoclinic and the systematic extinctions: $h0l$, $l = 2n + 1$; $0k0, k = 2n + 1$ leading to the space group $P2_1/c$ (n° 14).

The unit cell parameters were determined accurately using an automatic four-circle Nonius CAD 4 diffractometer by centering on 23 reflections with θ values of about 10° and refining by least-square techniques.

Crystal data

$TlZrF_5$, $M = 390.58$, $a = 8.112(1)$ Å, $b = 7.927(3)$ Å, $c = 7.929(1)$ Å, $\beta = 123.99(1)°$, $D_m = 6.12$ g/cm^3, $D_c = 6.14$ g/cm^3 for $Z = 4$.

Intensity Measurements

Intensity measurements were made on a crystal with approximate dimensions: 0.015 × 0.116 × 0.025 mm. Data were collected using an $\omega - 2\theta$ scan technique and MoK_α radiation monochromated with a flat graphite monochromator crystal ($\lambda = 0.71069$ Å). Three reflections measured at 120-mn intervals showed no systematic variation in intensity (the relative standard deviation is 0.02) and the orientation was checked after every 200 reflections. Intensities of 1834 reflections were registered in the FLAT[1] mode over the range $1 < \theta < 35°$ and reduced to 1140 with $I > 3\sigma(I)$. Lorentz and polarization corrections were applied, followed by an absorption correction ($\mu = 410.46$ cm^{-1}) made with the program AGNOST using the De Meulaner and Tompa's analytical method (*17*) (minimum absorption correction 0.231, maximum 0.517).

Structure Solution and Refinement

The thallium atom position was deduced from the Patterson function and calculation of structure factors resulted in $R = \Sigma$

[1] In the FLAT mode, the controlling program calculates the position of minimum absorption for each reflection from the input vector (perpendicular to the plate) and rotates the crystal about the scattering vector to reach the position nearest to the optimum.

TABLE I

FINAL VALUES OF ATOMIC AND THERMAL PARAMETERS ($\times 10^4$)[a,b] FOR $TlZrF_5$

Atom	Position	x	y	z	B_{eq} ($Å^2$)
Tl	4e	690(2)	284(2)	2715(2)	2.2
Zr	4e	4920(4)	6634(3)	3311(3)	0.4
F(1)	4e	2238(22)	2085(19)	626(22)	0.8(.2)
F(2)	4e	4883(22)	7078(19)	545(21)	0.8(.2)
F(3)	4e	3259(21)	4936(19)	3977(21)	0.9(.2)
F(4)	4e	2017(27)	7073(24)	1164(27)	1.7(.3)
F(5)	4e	5046(24)	4370(21)	2150(24)	1.4(.3)

	β_{11}	β_{22}	β_{33}	β_{12}	β_{13}	β_{23}
Tl	100(2)	109(2)	126(3)	−30(3)	50(2)	−25(3)
Zr	39(4)	7(3)	14(4)	1(3)	20(3)	−2(3)

[a] Standard deviations are given in parentheses.

[b] The β_{ij} have dimensions $Å^2$. The expression for the thermal factor is: $\exp[-(h^2\beta_{11} + k^2\beta_{22} + l^2\beta_{33} + 2hk\beta_{12} + 2hl\beta_{13} + 2kl\beta_{23})]$.

$|F_o| - |F_c| / \Sigma |F_o| = 0.316$. A Fourier synthesis enabled the zirconium atom to be located. Two subsequent cycles of refinement of the cationic positions lead to an R value of 0.16. With this data a difference Fourier synthesis revealed the positions of the five independent fluorine atoms. Subsequent full-matrix least-squares refinements and use of isotropic thermal parameters gave $R = 0.086$. The scattering factors for Tl^+, Zr^{4+}, and F^- ions were taken from the "International Tables for X-Ray Crystallography" (*18*), as were the anomalous dispersion terms for Tl and Zr for Mo$K\alpha$ radiation. Final refinement in which only the cations were assigned anisotropic thermal parameters led to $R = 0.057$ ($\omega R = [\Sigma \omega(|F_o| - |F_c|)^2 / \Sigma \omega F_o^2]^{1/2} = 0.063$). The final parameters with their estimated standard deviations are listed in Table I.

A list of the observed and calculated structure factors can be requested from the authors.

Description of the Structure and Discussion

The Zr^{4+} ion is coordinated by 8 F^-. The coordination polyhedron may be described as a triangular prism with pyramids on two of the prism faces similar to that reported by Brunton for the U^{4+} coordination in Li_4UF_8 (*19*). The Zr–F distances are presented in Table II. The structure consists of sheets of $(ZrF_5)^-$ built of ZrF_8 polyhedra in which an edge (involving F(3)–F(3)) is shared with an adjacent polyhedron and four corners [F(2) or F(5)] are shared with four additional polyhedra. The sheets run parallel to the (100) plane (see Figs. 1 and 2). The remaining corners [F(1) and F(4)] of each polyhedron are unshared and lie on the surface of the sheet. These two unshared fluorines are involved in the two shortest Zr–F bonds, respectively 1.996 and 2.022 Å. The sheets are bound together by thallium ions which are coordinated by 12 F^-. The Tl–F distances in this polyhedron range from 2.706 to 3.476 Å.

In the presently known fluoro complexes

TABLE II

INTERATOMIC DISTANCES (Å) IN $TlZrF_5$

Tl–F(3)	2.706(16)	Zr–F(1)	1.996(17)
Tl–F(1)	2.834(15)	Zr–F(4)	2.022(16)
Tl–F(1)	2.945(21)	Zr–F(5)	2.049(18)
Tl–F(4)	2.973(20)	Zr–F(2)	2.058(19)
Tl–F(1)	3.022(13)	Zr–F(3)	2.169(19)
Tl–F(4)	3.131(25)	Zr–F(3)	2.191(14)
Tl–F(4)	3.260(23)	Zr–F(5)	2.201(17)
Tl–F(5)	3.321(13)	Zr–F(2)	2.206(20)
Tl–F(4)	3.333(17)		
Tl–F(2)	3.360(17)		
Tl–F(2)	3.405(14)		
Tl–F(5)	3.476(22)		
F(1)–F(3)	2.481(27)	F(3)–F(3)	2.346(28)
F(1)–F(2)	2.598(17)	F(3)–F(4)	2.522(24)
F(1)–F(5)	2.619(22)	F(3)–F(5)	2.599(32)
F(1)–F(5)	2.874(21)	F(3)–F(5)	2.630(23)
F(1)–F(4)	2.980(26)	F(4)–F(5)	2.686(25)
F(2)–F(5)	2.454(28)		
F(2)–F(5)	2.467(24)		
F(2)–F(5)	2.552(26)		
F(2)–F(3)	2.625(22)		
F(2)–F(4)	2.632(34)		
F(2)–F(3)	2.655(20)		
F(2)–F(4)	2.983(21)		

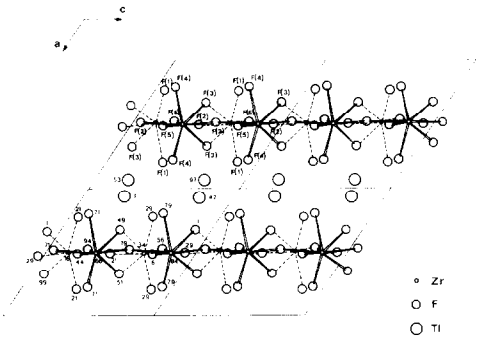

FIG. 1. Projection of the structure on the (010) plane. Numbers appearing on the lower left unit cell are the positions on the b axis ($\times 10^2$).

formed between zirconium tetrafluoride and the alkali fluorides as well as the ammonium and thallous fluorides, the Zr^{4+} ion is surrounded by six, seven, or eight fluorine ions.

Of the seven 8-coordination polyhedra possible (*20*) the Zr^{4+} ion adopts only three of them in the fluoride compounds known at present, namely, the square antiprism with idealized symmetry (D_{4d}), the dodecahedron (D_{2d}), and the bicapped trigonal prism (C_{2v}). This last is the fifth in the repulsivity scale defined by King (*21*) and was found for the first time in $TlZrF_5$.

Such a polyhedron is considerably higher in energy than either of the more usual 8-coordination polyhedra, and it is easy to predict that there will be but few representatives in this structural type. Attempts have been made to synthesize other related fluorides from Tl with tetravalent elements having close ionic radii (M^{4+} = Sn, Tb, Hf), but were successful only for Hf. Cell parameters for $TlHfF_5$ are a = 8.071 Å, b = 7.866 Å, c = 7.892 Å, β = 123.33°. X-Ray powder patterns for both $TlZrF_5$ and $TlHfF_5$ are given in Table III.

It can be seen from Fig. 1 that both the F(1) and F(4) atoms are different from the other fluorine atoms from the point of view of bonding. They lie on each side of the $(ZrF_5)^-$ sheet, while F(2), F(3), and F(5) are involved in the shared edges and corners. This suggests the possibility of ion exchange properties and for this reason the ionic conductivity of both $TlZrF_5$ and $TlHfF_5$ has been investigated.

Conductivity Results

Conductivity measurements were made using ion-blocking electrodes to determine the magnitude of the conductivity. No significant difference was found between measurements using Au or Pt as electrode materials, nor for samples of different thicknesses.

The impedance data were analysed using a complex impedance plot. Typical complex impedance diagrams obtained for $TlZrF_5$ are presented in Fig. 3. The maximum frequency of the impedance measurement system is not high enough to determine the high-frequency semicircle.

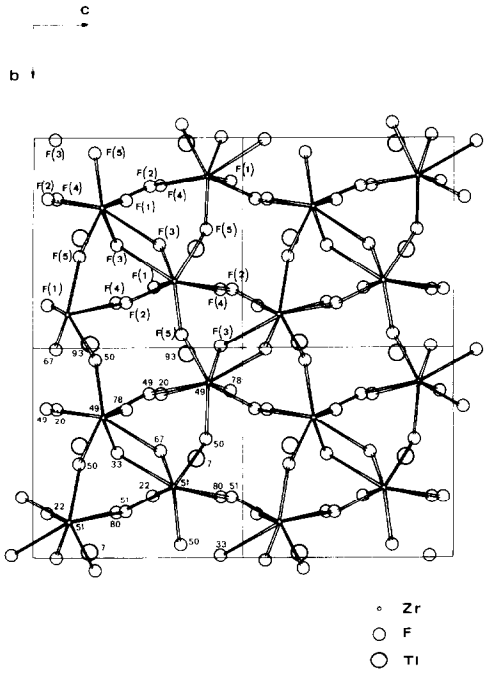

FIG. 2. Projection of the structure on the (100) plane. Numbers appearing on the lower left unit cell are the positions on the a axis ($\times 10^2$).

TABLE III

X-RAY POWDER DATA FOR $TlZrF_5$ AND $TlHfF_5$

$TlZrF_5$				$TlHfF_5$			
d_{obs} (Å)	d_{calc} (Å)	$h\ k\ l$	I/I_0	d_{obs} (Å)	d_{calc} (Å)	$h\ k\ l$	I/I_0
6.70	6.72	1 0 0	1	6.76	6.74	1 0 0	1
3.96	3.97	0 2 0	33	3.93	3.93	0 2 0	12
3.60	3.61	2 1 $\bar{1}$	34	3.58	3.59	2 1 $\bar{1}$	28
3.53	3.54	$20\bar{2}$–$11\bar{2}$	42	3.50	3.52 3.51	1 1 $\bar{2}$ 2 0 $\bar{2}$	56
3.41	3.42 3.40 3.40	1 2 0 1 1 1 0 2 1	100	3.39	3.41 3.40 3.38	1 1 1 1 2 0 0 2 1	100
3.28	3.29	0 0 2	32	3.30	3.30	0 0 2	31
3.22	3.23	2 1 $\bar{2}$	13	3.20	3.21	2 1 $\bar{2}$	19
3.05	3.04	0 1 2	8	3.04	3.04	0 1 2	16
2.829	2.833	2 2 $\bar{1}$	11	2.815	2.815	2 2 $\bar{1}$	9
2.798	2.799	1 2 $\bar{2}$	52	2.778	2.782	1 2 $\bar{2}$	46
2.637	2.640	2 2 $\bar{2}$	15	2.614	2.619	2 2 $\bar{2}$	7
2.560	2.564	2 2 0	13				
2.531	2.531	0 2 2	23	2.529	2.527	0 2 2	9
2.485	2.483	3 1 $\bar{1}$	26	2.475	2.477	3 1 $\bar{1}$	20
2.372	2.370	2 1 1	15	2.383	2.380	2 1 1	10
2.259	2.261	3 1 $\bar{3}$	8	2.362	2.360	1 1 2	4
2.239	2.241	3 0 0	8	2.249	2.248	3 0 0	12
2.212	2.213	2 3 $\bar{1}$	6	2.172	2.175	$22\bar{3}$–$32\bar{1}$	5
2.191	2.190	2 2 $\bar{3}$	7	2.114	2.117	0 1 3	11
2.142	2.141	1 2 $\bar{3}$	6	2.102	2.101	2 3 $\bar{2}$	8
2.111	2.112	0 1 3	8	2.093	2.094	1 2 2	10
2.105	2.105	2 2 1	9	2.014	2.016 2.012	4 0 $\bar{2}$ 3 2 $\bar{3}$	1
2.028	2.028 2.024	3 2 $\bar{3}$ 4 0 2	8	1.955	1.953	4 1 $\bar{2}$	14
1.981	1.983	0 4 0	13	1.925	1.927	3 0 $\bar{4}$	15
1.961	1.961	4 1 2	10	1.909	1.909	2 1 $\bar{4}$	12
1.939	1.940	3 0 $\bar{4}$	11	1.895	1.895 1.894 1.894	4 1 $\bar{3}$ 2 0 2 1 4 $\bar{1}$	64
1.909	1.909	$14\bar{1}$–$41\bar{3}$	34				
1.882	1.883	2 0 2	7				
1.854	1.853	1 0 $\bar{4}$	32	1.853	1.853	1 0 $\bar{4}$	42

However, one can still obtain the electrolyte resistance from the low-frequency intercept with the real axis. Although no measurement has been carried out, the possibility of electronic conductivity can be discounted. Such measurements were made in several binary fluorides and showed that the electronic conductivity is negligible (*10, 12, 22*).

The temperature dependence of the conductivity for both $TlZrF_5$ and $TlHfF_5$ is shown in Fig. 4. It is conventional to plot $\log(\sigma T)$ versus T^{-1}, but here measurement results are plotted as $\log \sigma$ versus $1/T$ for convenience and because it provides linear plots for the data (*23, 24*). For both $TlZrF_5$ and $TlHfF_5$ the data reveal a low-conductivity activation energy of 0.30 eV. which

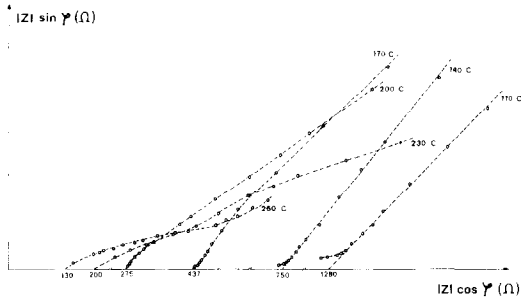

FIG. 3. Complex impedance diagrams for $TlZrF_5$ pressed pellets between blocking gold electrodes. Frequencies are indicated on the plot in hertz.

may be anticipated from the large polarizability of Tl^+. The measured conductivity of $TlHfF_5$ is always lower than that of $TlZrF_5$, but this is probably due to the difference of electronegativity between Hf and Zr.

Relationship between Structure and Ionic Conductivity in the Pentafluorozirconate of Thallium

It is now well known that fast-ionic conduction is a phenomenon extremely sensitive to crystallographic considerations. Some time ago it was pointed out by Huggins (*25*) that the dominant factor cannot be the presence of an unusually large concentration of the mobile species. Instead, the most important factors relate to the geometry of the static part of the crystal structure and the potential energy profiles along which the mobile ions move. Inspection of the structure of $TlZrF_5$ reveals that thallium and zirconium polyhedra are joined into a three-dimensional framework by sharing corners, edges, and faces. This arrangement produces relatively open tunnels in the *b* direction, delimited by the cations, as shown in Fig. 5 by the dashed line. As mentioned above it is probably not unreasonable to suppose that the most weakly bound fluorine atoms, namely, F(1) and F(4) are primarily responsible for the high conductivity of this material. Although both F(1) and F(4) are involved in the two shortest Zr–F distances they have the lowest electrostatic valences. Thus it would not be surprising for them to move rapidly along the [010] direction within the tunnel and even exchange between themselves along and across this tunnel. If such a

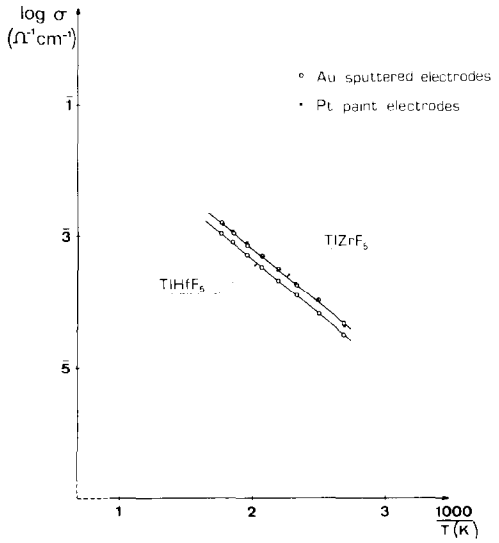

FIG. 4. Thermal variation of the ionic conductivity of both $TlZrF_5$ and $TlHfF_5$ plotted as log σ versus the inverse of the absolute temperature.

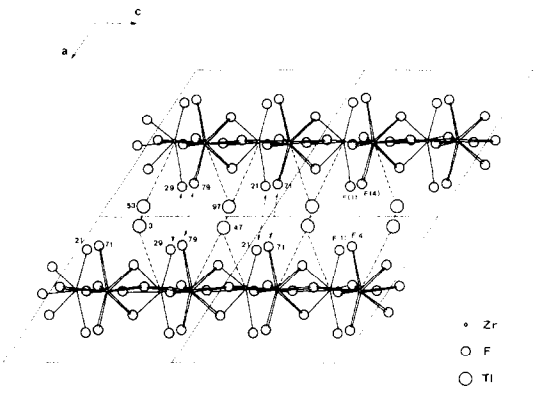

FIG. 5. An illustration of the $TlZrF_5$ structure in the [010] direction. The dashed lines show the tunnels delimited by the cations, Zr and Tl, within which both F(1) and F(4) might move and exchange between themselves.

mechanism occurs the ionic conductivity would be very anisotropic. Further speculation on the conduction mechanism does not seem warranted before complementary measurements.

Attempts to grow a large single crystal of $TlZrF_5$ is currently in progress in order to carry out anisotropic measurements of the ionic conductivity.

References

1. L. E. Nagel and M. O'Keeffe, *in* "Fast Ion Transport in Solids" (W. Van Gool Ed.), p. 165, North-Holland, Amsterdam (1973).
2. J. M. Reau, J. Claverie, G. Campet, C. Deportes, D. Ravaine, J. L. Souquet, and A. Hammou, *C. R. Acad. Sci. Paris Ser. C* **280**, 325 (1975).
3. J. M. Reau, C. Lucat, G. Campet, J. Portier, and A. Hammou, *J. Solid State Chem.* **17**, 123 (1976).
4. C. Lucat, G. Campet, J. Claverie, J. Portier, J. M. Reau, and P. Hagenmuller, *Mater. Res. Bull.* **11**, 167 (1976).
5. J. Schoonmann, G. J. Dirkson, and R. W. Bonne, *Solid State Commun.* **19**, 783 (1976).
6. C. Lucat, P. Sorbe, J. Portier, J. M. Reau, P. Hagenmuller, and J. Grannec, *Mater. Res. Bull.* **12**, 145 (1977).
7. A. V. Joshi and C. C. Liang, *J. Electrochem. Soc.* **124**, 1253 (1977).
8. T. Takahashi, H. Iwahara, and T. Ishikawa, *J. Electrochem. Soc.* **124**, 280 (1977).
9. J. M. Reau, A. Rhandour, C. Lucat, J. Portier, and P. Hagenmuller, *Mater. Res. Bull.* **13**, 827 (1978).
10. J. M. Reau, C. Lucat, J. Portier, P. Hagenmuller, L. Cot, and S. Vilminot, *Mater. Res. Bull.* **13**, 877 (1978).
11. C. Lucat, A. Rhandour, J. M. Reau, and P. Hagenmuller, *Ann. Chim. Fr.* **3**, 279 (1978).
12. J. Schoonman, K. E. D. Wapenaar, G. Oversluizen, and G. J. Dirksen, *J. Electrochemical Soc.* **126**, 709 (1979).
13. J. M. Reau, J. Portier, A. Levasseur, G. Villeneuve, and M. Pouchard, *Mater. Res. Bull.* **13**, 1415 (1978).
14. J. M. Reau and J. Portier, *in* "Solid Electrolytes" (P. Hagenmuller and W. Van Gool, Eds.), Chap. 19, Academic Press, New York (1978).
15. D. Avignant and J. C. Cousseins, *C.R. Acad. Sci. Paris Ser. C* **274**, 631 (1972).
16. D. Avignant, I. Mansouri, R. Sabatier, and J. C. Cousseins, *Ann. Chim. Fr.* **8**, 585 (1979).
17. De Meulaner and Tompa, *Acta Crystallogr.* **19**, 1014 (1965).
18. "International Tables for X-Ray Crystallography," Vol. 4, Birmingham, Kynoch Press (1968).
19. G. Brunton, *J. Inorg. Nucl. Chem.* **29**, 1631 (1967).
20. E. L. Muetterties and C. M. Wright, *Quart. Rev.* **21**, 109 (1967).
21. R. B. King, *J. Amer. Chem. Soc.* **92**(22), 6455 (1970).
22. D. Ansel and J. DeBuigne, *C.R. Acad. Sci. (Paris) Ser C* **287**, 451 (1978).
23. P. H. Bottelberghs, *in* "Solid Electrolytes" (P. Hagenmuller and W. Van Gool, Eds.), Chap. 10, Academic Press, New York (1978).
24. C. E. Derrington, A. Lindner, and M. O'Keeffe, *J. Solid State Chem.* **15**, 171 (1975).
25. R. A. Huggins, *in* "Diffusion in Solids: Recent Developments" (A. S. Nowick and J. J. Burton, Eds.), p. 445, Academic Press, New York (1975).